AJNR

Diffusion imaging of the human brain: a new pulse sequence application for a 1.5-T standard MR system.

K Harada, N Fujita, K Sakurai, Y Akai, K Fujii and T Kozuka

This information is current as of April 17, 2024.

Diffusion Imaging of the Human Brain: A New Pulse Sequence Application for a 1.5-T Standard MR System

Koushi Harada[1]
Norihiko Fujita
Kousuke Sakurai
Yoshinori Akai
Keiko Fujii
Takahiro Kozuka

We developed a new pulse sequence and investigated whether the anisotropic diffusion in the human brain can be detailed with a standard whole-body MR imager. Apparent diffusion coefficient maps were produced by the proposed sequence using a 1.5-T MR unit. The sequence employed simultaneous application of three orthogonal gradients to achieve an optimal signal attenuation for imaging the brain without any increase in echo time. The orientation of the effective diffusion-encoding gradient was off-axis. On the in vivo apparent diffusion coefficient maps of four healthy volunteers, white matter tracts (the internal capsule and the corpus callosum) and the cortical and deep white matter showed anisotropic diffusion. In the gray matter, such as basal ganglia and thalami, anisotropic diffusion was not observed.

A typical whole-body imager can provide in vivo human brain diffusion images of clinical quality. This technique has promising implications for the evaluation of brain development and the diagnosis of degenerative diseases.

MR diffusion imaging has been attracting increased interest in recent years [1–6]. One of the promising capabilities of this imaging method is in vivo visualization of the orientation of white matter fibers through anisotropic diffusion. Moseley et al. [4] obtained clear images of anisotropic diffusion in cats' brains and spinal cords using an experimental MR system. The presence of anisotropic diffusion was also demonstrated in the human brain by Chien et al. [5] using a whole-body clinical imaging unit. In general, however, the quality of in vivo human diffusion images has been less than optimal.

In this study, we developed a pulse sequence that employed simultaneous application of three orthogonal gradients and investigated whether the anisotropic diffusion in the human brain can be detailed with a typical whole-body MR system.

Materials and Methods

Pulse Sequence Description

Two spin-echo sequences were acquired: diffusion-sensitive and nonsensitive. The apparent diffusion coefficient (ADC) was calculated for each pixel on the basis of the signal intensities in order to generate an ADC map. The b value (the value of the gradient attenuation factor) [6] of the diffusion-nonsensitive sequence was calculated to be 3 sec/mm^2. It was much smaller than that of the diffusion-sensitive sequence. Hence, this value could be ignored, and the ADC for each pixel was calculated according to

$$ADC(x,y) = \ln[S_{off}(x,y)/S_{on}(x,y)]/b_{on},$$

where S_{off} and S_{on} are signal intensities of the diffusion-nonsensitive and sensitive sequences, respectively, and b_{on} is the b value of the diffusion-sensitive sequence [6, 7].

To obtain sufficient attenuation due to diffusion without increasing echo time, under the limited maximum strength of the gradient that was achievable with the available imager,

[1] All authors: Department of Radiology, Osaka University Medical School, 1-1-50, Fukushima, Fukushima-ku, Osaka 553, Japan. Address reprint requests to K. Harada.
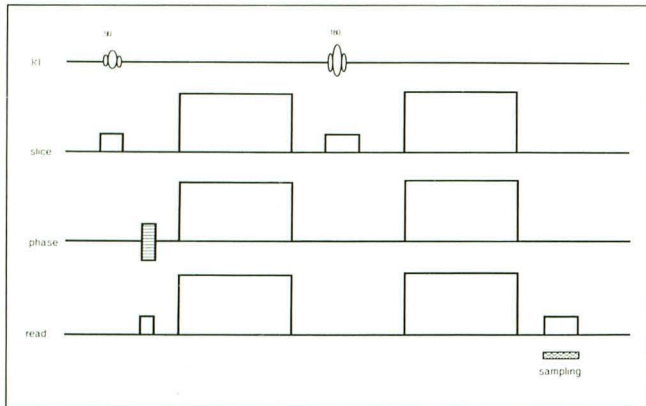
Fig. 1.—Diffusion-sensitive sequence. In all three axes, additional gradients are placed before and after the 180° pulse; all have the same duration and amplitude.

Fig. 2.—Effective diffusion-encoding gradient. The effective gradient is the vectorial addition of the three gradients. *Largest arrow* is the effective gradient; *smaller arrows* are actually applied gradients in frequency, phase-encoding, and slice-selective axes.

we developed a diffusion-sensitive sequence that simultaneously employs three orthogonal gradients. Gradients were placed in all three axes before and after the 180° pulse. They had the same duration and amplitude (Fig. 1). The effective diffusion-encoding gradient is the vectorial addition of the three gradients (Fig. 2). The strength is the square root of three times that of one gradient. Hence, the pulse sequence is three times more efficient in diffusion effects, since the latter are proportional to the square of the gradient strength.

The orientation of the effective gradient is oblique to all three of the orthogonal planes (Fig. 2); that is, from the left anterior caudad to the right posterior cephalad of examinees. On the other hand, the structure of the human brain is virtually symmetric against the sagittal plane. Therefore, if anisotropic diffusion is present in a pair of left and right white matter pathways that run obliquely against a sagittal plane, such as corticospinal tracts running through internal capsules and forceps minor, the pathways are expected to appear assymetric with different areas of brightness on an ADC image acquired by our method. Those white matter pathways that are not parallel to the orientation of the effective diffusion-encoding gradient will appear different from fiber tracts that are parallel.

Although the maximum gradient strength achievable with our system is 10 mT/m, the amplitude of the additional gradients was set to 8 mT/m because the use of a stronger amplitude increased the dynamic instrumental instabilities (gradient oscillations and vibration of gantry, couch, etc.).

The diffusion-sensitive sequence was optimized for a two-point fit calculation of the ADC of the human brain so as to minimize the measurement error. The optimization was achieved by controlling the duration of the diffusion-encoding gradient [8]. As a result, the duration was determined to be 30 msec. The b value for the diffusion-sensitive sequence was calculated to be 600 sec/mm^2 (b_s = 213, b_f = 195, b_p = 192 if phase encoding had not been performed) [7].

Phantom Studies

The accuracy of the diffusion measurements was tested with a water phantom at room temperature (23°C). ADC images, 500/120/1 (TR/TE/excitation), were obtained. The other imaging parameters used in the experiments were as follows: slice thickness = 10 mm, field of view = 23 cm, acquisition matrix = 128 × 256, and single slice acquisition.

To test the utility of our imaging method in the assessment of anisotropic diffusion, two axial ADC images (500/120/1) of a fresh
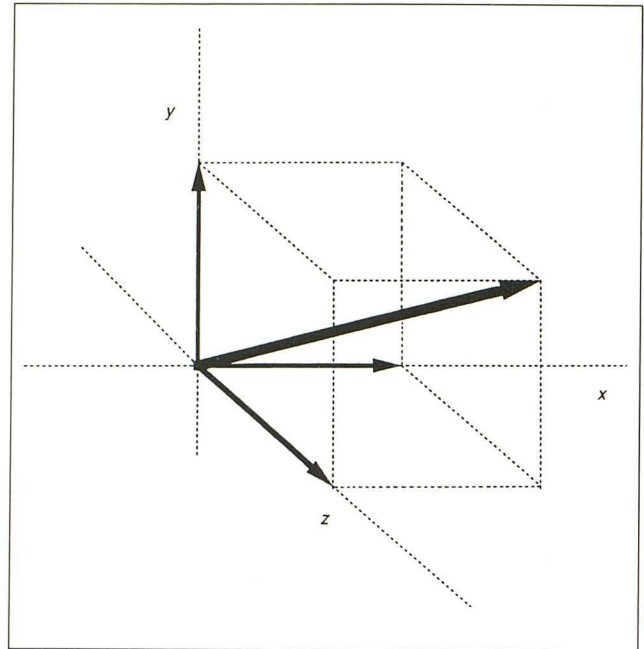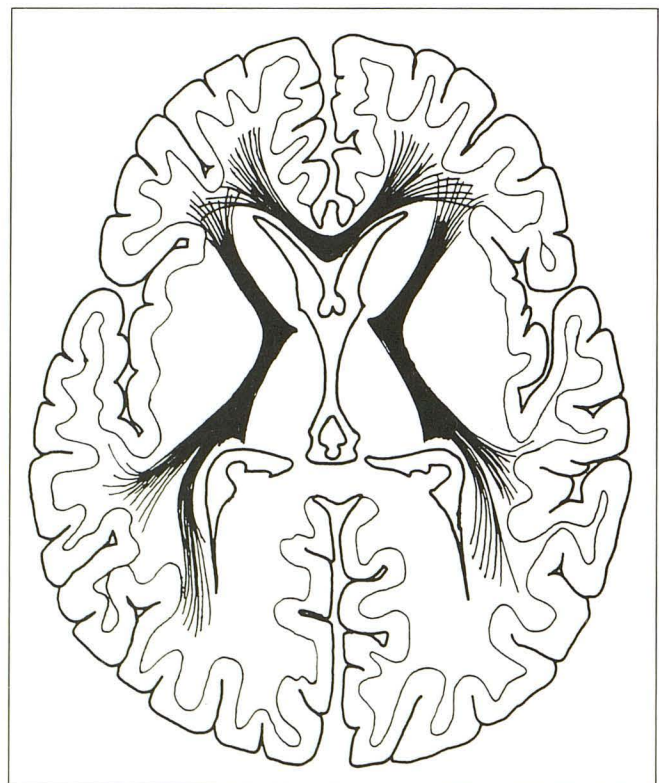

Fig. 3.—Imaging plane. Fibers of forceps minor form connections of the cortex of both frontal lobes through genu of corpus callosum. They run in an anterolateral direction from the lateral aspect of the genu. Most of the fibers of the internal capsules run obliquely through the plane. The fibers of the anterior thalamic peduncle and frontopontine tracts project into frontal lobes from the anterior limbs of the internal capsules.

pineapple were obtained with and without changing the orientation of the effective diffusion-encoding gradient (normal-direction and reversed-direction gradient images) [4, 5, 9]. The change of the orientation was achieved by the reversal of the gradient's polarity in the frequency axis (left-right direction on the ADC images). The imaging parameters were the same as those used in the water phantom study.

Normal Patient Studies

Human brain studies were performed in four healthy volunteers ages 28–39 years old. A transverse plane through the basal ganglia and thalamus was imaged in each subject. The reasons for selecting this plane were as follows: (1) the plane includes deep gray matter as well as deep white matter; (2) there is an internal capsule in which projection fibers run obliquely through the plane; and (3) it includes the genu of the corpus callosum and the forceps minor, whose fibers run obliquely within the plane (Fig. 3). The imaging parameters were the same as those used in the water phantom study except for TR and excitations. In the human studies, ECG-gated ADC images (3R-R/120/2) were obtained. The effective TRs were about 3000 msec. Averaging was performed by adding separately calculated images, because averaging of sequentially recorded image data is superior to direct averaging of data from individual phase-encoding steps [10].

The regional ADCs were measured by region-of-interest (ROI) operation on the normal-direction gradient images. The areas of the ROI were 0.5 cm^2 for the caudate head, putamen, thalamus, and frontal white matter; and 0.2 cm^2 for the corpus callosum and internal capsule. On measuring the ADC of the right posterior limb of the internal capsule, the ROI was placed over the brightest area.

To confirm direction dependence of diffusion—that is, anisotropic diffusion of the human brain—we changed the orientation of the effective diffusion-encoding gradient in the same way as described above. The resulting orientation was from the right anterior caudad to the left posterior cephalad of examinees. In two of the volunteers, an additional ECG-gated ADC image (3R-R/120/2) of the same transverse plane was produced by the proposed method with the reversed-direction gradient. The ADC images were compared with corresponding normal-direction gradient images.

All studies were acquired on a 1.5-T whole-body MR unit (Siemens, Erlangen, Germany) without special hardware modifications. The gradient system was not a shielded-gradient type.

Results

The diffusion coefficient of water measured by the proposed sequence with normal- and reversed-direction gradients in the frequency axis was 2.28 ± 0.03 and 2.27 ± 0.02 × 10^{-3} mm^2/sec, respectively, showing close agreement with each other. These diffusion coefficients are compatible with previously reported values [5–7].

On the normal-direction gradient ADC image (500/120) of the pineapple, which consists of a central fibrous core and
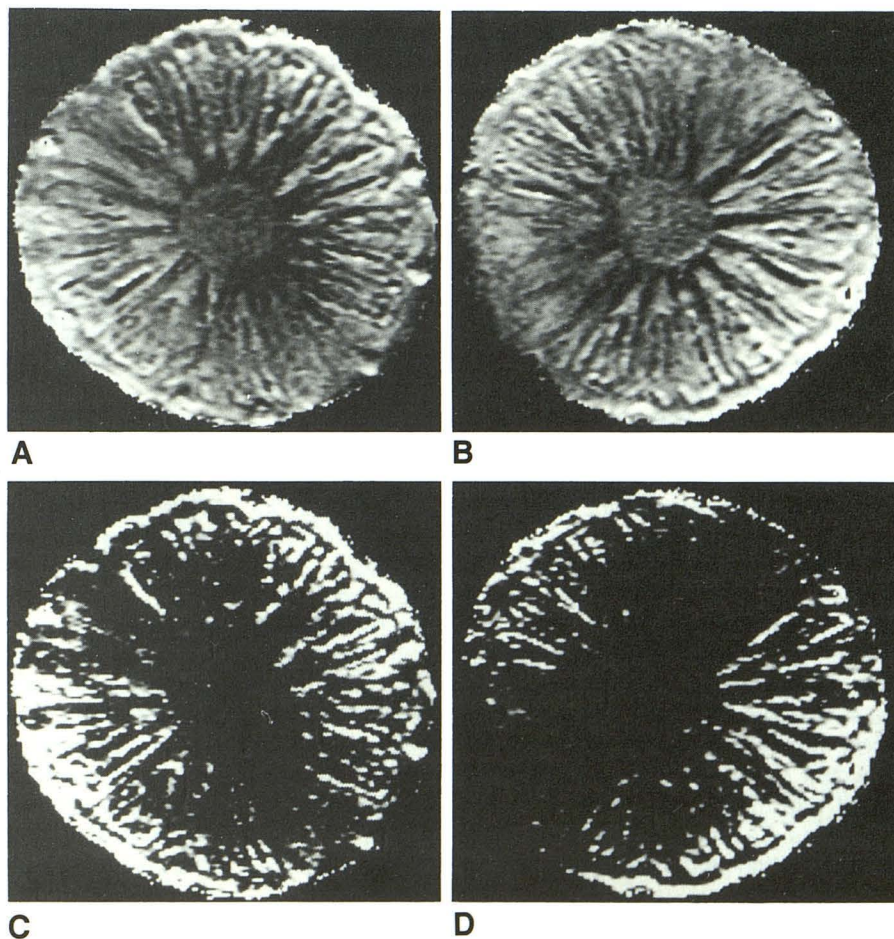

Fig. 4.—Apparent diffusion coefficient (ADC) images (500/120) of a pineapple. There is marked direction dependency of the images. On the normal-direction gradient image, faster ADC area (brighter on the image) runs from upper left to lower right region of the pineapple. Conversely, it moves from the upper right to the lower left region of the pineapple on the reversed-direction gradient ADC image.

A, Normal-direction gradient ADC image.
B, Reversed-direction gradient ADC image.
C and *D*, Display window is narrowed down from images *A* and *B*, respectively.

TABLE 1: Apparent Diffusion Coefficients on the Normal-Direction Gradient Images

Region	Volunteer				Average
	A	B	C	D	
Putamen					
L	44	72	93	61	68
R	83	56	74	83	74
Caudate					
L	63	82	84	66	74
R	62	54	70	69	64
Thalamus					
L	31	71	68	70	60
R	63	84	91	75	78
Posterior limb of internal capsule					
L	30	70	65	56	55
R	119	120	129	103	118
Genu of corpus callosum					
L	131	90	150	141	128
R	48	36	58	46	47
Frontal white matter					
L	101	87	111	129	107
R	63	64	82	57	67

Note.—L = left, R = right. All coefficients calculated by the equation ($\times 10^{-5}$ mm^2/sec).

radiating juicy fibrous columns around it, an asymmetric diffusion pattern against the midline was observed. Part of the fruit, where the fibrous columns run more closely parallel to the effective diffusion-encoding gradient, showed faster diffusion (brighter on the image) (Figs. 4A and 4C). On the reversed-direction gradient image, the diffusion pattern was reversed against the midline (Figs. 4B and 4D). These facts demonstrate that our imaging method can reflect the direction dependency of diffusion on image contrast and illustrate the presence of anisotropic diffusion.

All ADC 3R-R/120 images of the volunteers were slightly degraded by phase-shift artifacts. The regional ADCs measured on the normal-direction gradient are summarized in Table 1.

On all of the normal-direction gradient ADC 3R-R/120 images of the volunteers, some white matter pathways showed conspicuously faster diffusion (brighter on the images) than the corresponding contralateral regions. These areas included the right posterior limb of the internal capsule, the right side of the splenium, and the left side of the genu of the corpus callosum (Table 1 and Fig. 5). The appearance of the cerebral white matter was asymmetric (Figs. 5 and 6A). It was particularly prominent in the frontal region. The ADCs of the bilateral frontal white matter were significantly different (Table 1). The gray matter, such as basal ganglia and thalami, did not show any significant difference between the cerebral hemispheres (Table 1 and Figs. 5 and 6A). The asymmetric diffusion pattern was thought to be due to anisotropic diffusion.

On the reversed-direction gradient ADC 3R-R/120 image of the two volunteers, the contrast characteristics of the left and right cerebral hemispheres were interchanged as compared with the corresponding normal-direction gradient images (Figs. 6A and 6B). This result confirmed that the asymmetric diffusion pattern was caused by diffusional anisotropy.
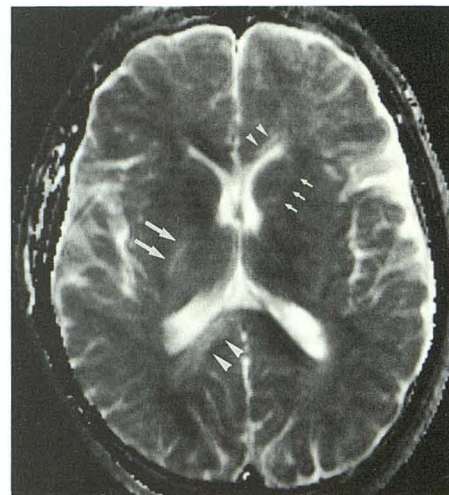

Fig. 5.—Normal-direction gradient apparent diffusion coefficient image (3R-R/120) of a healthy volunteer. The following regions reveal faster diffusion (brighter on the image) than the contralateral correspondents: the right posterior limb of the internal capsule (*large arrows*), the left anterior limb (*small arrows*), the right side of the splenium of the corpus callosum (*large arrowheads*), and the left side of the genu (*small arrowheads*). Difference in diffusion pattern is observable between the left and right frontal region.

Discussion

Although efforts have been made to improve diffusion imaging [7, 11–13] (Chenervert TL. Paper presented at the annual meeting of the Society of Magnetic Resonance in Medicine, Amsterdam, August 1989), in vivo measurements are highly susceptible to motion artifacts. These artifacts are caused by patient motion, CSF pulsation, brain tissue pulsation, and dynamic instrumental instabilities caused by the use
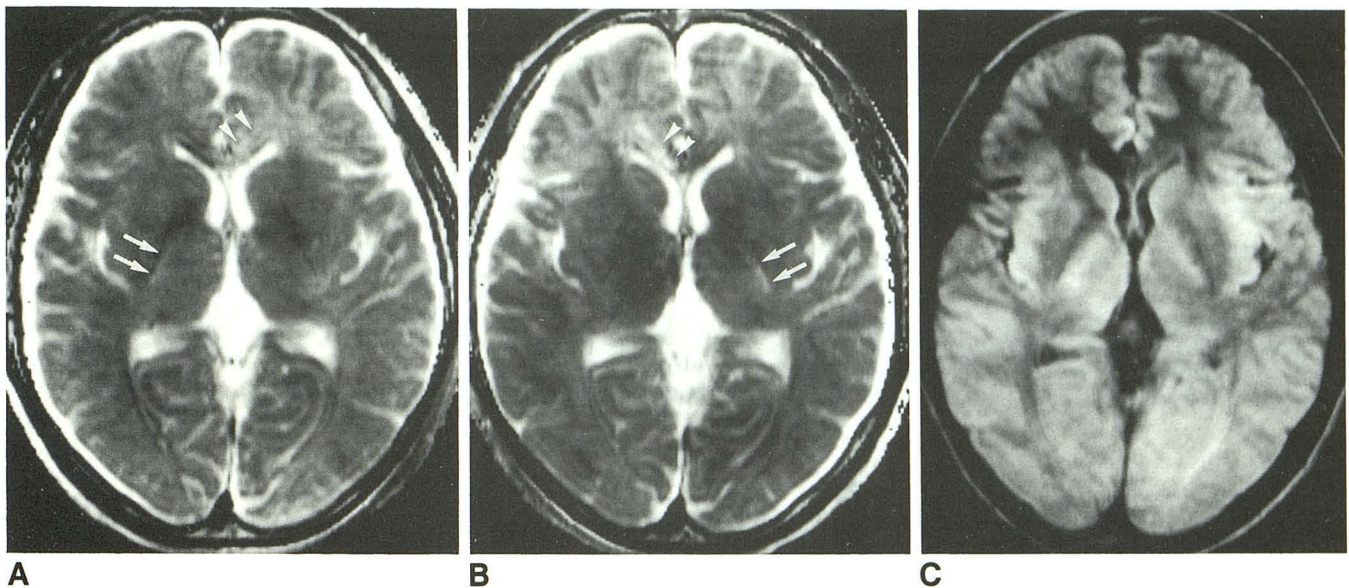
A   **B**   **C**

Fig. 6.—Apparent diffusion coefficient (ADC) maps and the diffusion-weighted image of a healthy volunteer.

A, Normal-direction gradient ADC image (3R-R/120). Right posterior limb of internal capsule (*arrows*) and left side of the genu of the corpus callosum (*arrowheads*) show faster diffusion (brighter on the image) than corresponding contralateral regions. The diffusion pattern was asymmetric in the frontal white matter. The gray matter, such as the basal ganglia and thalami, does not show any significant difference between the cerebral hemispheres.

B, Reversed-direction gradient ADC image (3R-R/120). Roughly, this is a mirror image of the normal-direction gradient image. Left posterior limb of internal capsule (*arrows*) and right side of the genu of the corpus callosum (*arrowheads*) reveal faster diffusion. There is no significant directional dependence in the gray matter.

of strong magnetic gradients. A relatively large, effective b value, used in the present study, suppresses phase-shift artifacts originating from CSF pulsation, because signal intensity of CSF considerably decreases owing to its high diffusion coefficient (Fig. 6C). The use of a large b value also improves tissue contrast [9]. A combination of single-slice acquisition and long TR was useful for reducing the effects of the dynamic instrumental instabilities.

Potentially, the ADC measured by our method reflects processes other than diffusion in living subjects, such as perfusion and physiological pulsation. The use of a large b value decreases the effects of perfusion on the ADC image. On the basis of the theory described by Le Bihan et al. [14, 15], the effects of perfusion on our diffusion measurements is estimated to be less than 8%. The effects of perfusion or physiological pulsation have been ruled out as the major cause of anisotropic diffusion in the white matter because of the similarity of premortem and immediate postmortem images [4].

Using a sequence that simultaneously employed three orthogonal gradients to sensitize diffusion, we detailed the diffusion pattern of the human brain. In the volunteer study, we demonstrated the anisotropic diffusion in the major white matter pathways and in the cortical and deep white matter. In the gray matter, such as the basal ganglia and thalami, anisotropic diffusion was not observed. These findings are in agreement with the results of earlier studies [4, 5, 9, 12, 13] (Nomura Y. Paper presented at the annual meeting of the

Society of Magnetic Resonance in Medicine, New York, August 1990).

In conclusion, a typical whole-body imager can provide an in vivo human brain diffusion image of clinical quality. Although much work remains to be done before we have a good understanding of anisotropic diffusion in the human brain, we think that the application of this technique is promising in the evaluation of brain development and the diagnosis of degenerative diseases.

REFERENCES

1. Wesbey GE, Moseley ME, Ehman RL. Translational molecular self-diffusion in magnetic resonance imaging. 2. Measurement of the self-diffusion coefficient. *Invest Radiol* **1984**; 19:491–498
2. Thomsen C, Henricksen O, Ring P. In vivo measurement of water self diffusion in the human brain by magnetic resonance imaging. *Acta Radiol* **1987**; 28:353–361
3. Tsuruda JS, Chew WM, Moseley ME, Norman D. Diffusion-weighted MR imaging of the brain: value of differentiating between extraaxial cysts and epidermoid tumors. *AJNR* **1990**; 11:925–931
4. Moseley ME, Cohen Y, Mintrovitch J, et al. Diffusion-weighted MR imaging of anisotropic water diffusion in cat central nervous system. *Radiology* **1990**; 176:439–445
5. Chien D, Buxton RB, Kwong KK, Brady TJ, Rosen BR. MR diffusion

imaging of the human brain. *J Comput Assist Tomogr* **1990**; 14:514–520

6. Le Bihan D, Breton E, Lallemand D, Greiner P, Cabanis E, Laval-Jeantet M. MR imaging of intravoxel incoherent motions: application to diffusion and perfusion in neurologic disorders. *Radiology* **1986**; 161:401–407

7. Ahn CB, Lee SY, Nalcioglu O, Cho ZH. An improved nuclear magnetic resonance diffusion coefficient imaging method using an optimized pulse sequence. *Med Phys* **1986**; 13:789–793

8. Hrovat MI, Wade CG. NMR pulsed gradient diffusion measurements. 2. Residual gradients and lineshape distortions. *J Magn Reson* **1981**; 45:67–80

9. Moseley ME, Cohen Y, Mintrovitch J, et al. Early detection of regional cerebral ischemia in cats: comparison of diffusion- and T2-weighted MRI and spectroscopy. *Magn Reson Med* **1990**; 14:330–346

10. Merboldt KD, Bruhn H, Frahm J, Gyngell ML, Haenicke W, Deimling M. MRI of "diffusion" in the human brain. New results using a modified CE-FAST sequence. *Magn Reson Med* **1989**; 9:423–429

11. Moseley ME, Kucharczyk J, Mintrovitch J, et al. Diffusion-weighted MR imaging of acute stroke: correlation with T2-weighted and magnetic susceptibility enhanced MR imaging in cats. *AJNR* **1990**; 11:423–429

12. Doran M, Hajnal JV, Van Bruggen N, King MD, Young IR, Bydder GM. Normal and abnormal white matter tracts shown by MR imaging using directional diffusion weighted sequences. *J Comput Assist Tomogr* **1990**; 14:865–873

13. Hajnal JV, Doran M, Hall AS, et al. MR imaging of anisotropically restricted diffusion of water in the nervous system: technical, anatomic, and pathologic considerations. *J Comput Assist Tomogr* **1991**; 15:1–18

14. Le Bihan D, Breton E, Lallemand D, Aubin ML, Vignaud J, Laval-Jeantet M. Separation of diffusion and perfusion in intravoxel incoherent motion MR imaging. *Radiology* **1988**; 168:497–505

15. Le Bihan D. Magnetic resonance imaging of perfusion. *Magn Reson Med* **1990**; 14:283–292